World Academy of Science, Engineering and Technology
International Journal of Environmental and Ecological Engineering
Vol:1, No:7, 2007

Analysis of Temperature Change under Global Warming Impact using Empirical Mode Decomposition

Md. Khademul Islam Molla, Akimasa Sumi and M. Sayedur Rahman

***Abstract*—** The empirical mode decomposition (EMD) represents any time series into a finite set of basis functions. The bases are termed as intrinsic mode functions (IMFs) which are mutually orthogonal containing minimum amount of cross-information. The EMD successively extracts the IMFs with the highest local frequencies in a recursive way, which yields effectively a set low-pass filters based entirely on the properties exhibited by the data. In this paper, EMD is applied to explore the properties of the multi-year air temperature and to observe its effects on climate change under global warming. This method decomposes the original time-series into intrinsic time scale. It is capable of analyzing nonlinear, non-stationary climatic time series that cause problems to many linear statistical methods and their users. The analysis results show that the mode of EMD presents seasonal variability. The most of the IMFs have normal distribution and the energy density distribution of the IMFs satisfies Chi-square distribution. The IMFs are more effective in isolating physical processes of various time-scales and also statistically significant. The analysis results also show that the EMD method provides a good job to find many characteristics on inter annual climate. The results suggest that climate fluctuations of every single element such as temperature are the results of variations in the global atmospheric circulation.

***Keywords*—**Empirical mode decomposition, instantaneous frequency, Hilbert spectrum, Chi-square distribution, anthropogenic impact.

I. Introduction

CLIMATE as a complex system still challenges our knowledge, leaving us with the problems that deal with sparse data, insufficient methods, limited models and unexplained physical processes [1]. Global warming is one of the most serious global environmental issues facing mankind. Climate is a fundamental component of the Earth's natural system. Effect of global warming is already visible. The global mean temperature has increased by 0.6^{o}C over the last century and many organisms and ecosystems have experienced changes. There is a perception that extreme natural disasters such as floods, droughts, and heat waves, have become more frequent. This change in climate plays an important role in the Earth's sustainability. The impact of hydrological change as a result of global warming caused by anthropogenic emissions of greenhouse gases is a fundamental concern [2]-[4]. In order to control water resources in the face of drought, flood and soil erosion, which frequently present a serious threat to human life and natural ecosystems, risk assessments are being required more frequently by policy makers [5].

Climate is currently changing in ways that mirror the effects of global warming [6]. There is also increasing demand for climate change information, particularly from policy makers for impact assessment studies [7]. Several linear statistical models have been applied to climate records, but the answers are not conclusive due to the high sensitivity of model results to model parameters [8]-[10], especially when stochastic processes are taken into account [11]. Various approaches have been employed to develop climate change scenarios at different scales [12]. In recent years, several weather events have caused large losses of life as well as a tremendous increase in economic losses from weather hazards. These life and property losses helped raise the alarm over the possibility that the recent increases were due to a shifting climate [13].

Geographical distribution of the change in annual mean surface air temperature rise is greater over continents than over oceans and greater in the Polar Regions than in tropical region. The features are consistent with previous studies. In the tropical Pacific, temperature rise is greater in the central-east part than in the western part. Such an anomaly pattern is observed in the El Nino years. The warming patterns among the scenarios are similar although the magnitudes are different [14]. Many critical impacts of climate are controlled by extreme events rather than mean values. Aspects of human activity and environment are usually well adjusted to mean climate conditions and show little sensitivity to moderate variations around these means. Systems that are particularly vulnerable are agricultural and forest ecosystems, coasts and water resources. High temperatures can exacerbate drought conditions. Very high temperature also damage crops and reduce yields. However, low temperatures are important to some temperate horticulture and cereal crops in promoting yield and development [15].

The surface runoff changes had regional differences and both

Manuscript received December 28, 2005.

Md. Khademul Islam Molla is with the Department of Frontier Informatics, The University of Tokyo, 7-3-1 Hongo, Bunkyo-ku, Tokyo 113-0033, Japan. (Tel: +81-3-5841-6767, e-mail: molla@gavo.t.u-tokyo.ac.jp).

Akimasa Sumi is with the Center for Climate System Research, The University of Tokyo, 5-15 Kashiwanoha, Kashiwa-shi, Chiba 277-8568, Japan. (e-mail: sumi@ccsr.u-tokyo.ac.jp).

M. Sayedur Rahman is with the Center for Climate System Research, The University of Tokyo, 5-15 Kashiwanoha, Kashiwa-shi, Chiba 277-8568, Japan. (e-mail: rahman@ccsr.u-tokyo.ac.jp).

the increase and decrease were suggested in summer. It might increase the risk of mismatch between water demand and water availability in the agricultural region. Under the global warming, both temperature and humidity were projected to increase in Asian region. The increases of annual mean surface runoff and its large fluctuations were projected in a lot of Asian regions. In some regions, the projected seasonal changes of hydrological cycles under the global warming potentially increase the risk of droughts and floods [16].

Coughlin and Tung [17] found that the atmosphere warms during the solar maximum almost everywhere over the globe. It should be pointed out that changes in the correlation values with latitude do not imply similar amplitude changes with latitude. However, the fact that the correlation with the solar flux is positive everywhere over the globe does imply that, on average, the temperatures increase during solar maxima at all latitudes. This makes the phenomenon difficult to explain with dynamical mechanisms involving over turning meridional circulations in the troposphere. This is useful information to atmosphere dynamicity wishing to come up with a mechanism for the influence of solar cycle variations on the lower atmosphere.

The El Nino and the southern oscillation phenomenon (ENSO) is the primary driver of inter-annual climate variability and have a large economic and social impact over the universe [18]. Fedorov and Philander [19] demonstrated that mean fluctuations of decadal timescale do contribute significantly to the later unusual ENSO events and suggested that global warming cannot be ruled out as a suspect [20]. El Nino like differences can be found in the projected results by the AGCM under global warming [21]. As a result of global warming, the stronger temperature increase in the higher latitudes, the meridional gradients of air temperature became weak and westerly caused by thermal wind were weakened.

Monsoon westerly in the Arabian Sea, which is associated with Somali jet, were projected to be stronger and to bring more abundant water vapor to the south of India and the Bay of Bengal. Under global warming, increase of water vapor and higher air temperature over the land than over the ocean were projected. It enhanced a giant land-sea breeze, Asian monsoon circulation. As a result of the changes in the synoptic scale flow patterns and precipitation under the global warming, the increase of annual mean surface runoff was projected in a lot of Asian regions [22].

A new non-linear technique, Empirical Mode Decomposition (EMD) has recently been pioneered by Huang [23] for adaptively representing non-stationary time series data. Although it proved remarkably effective the technique is faced with the difficulty of being essentially defined by an algorithm and therefore does not admitting an analytical formulation which would allow for a theoretical analysis and performance evaluation [23], [24]. In this study will attempt to obtain a better understanding of the variability of the regional climate measured by the changes in the surface air temperature. By applying several statistical techniques, including EMD analysis, the output of the study will document the detail features of the variability of temperature on various time scales.

II. Data and Methodology

The following data sets have been used for this study. Daily minimum and maximum temperature data for adjoining areas in the Giridhi, Bihar, India were collected from Indian Statistical Institute (ISI), Kolkata database, for the period 1989 to 2004. All the weather parameters were measured with instruments specified by Indian Meteorological Department, Govt. of India. Climatologically, the area under study is located in the tropical Indian monsoon region. The climate of the area before the monsoon is characterized by a hot summer seasons, this is called pre-monsoon season. However in early March, the area also experiences the impact of western disturbances, resulting in significant rainfall. The main source of rainfall in March is the pre-monsoon thunderstorm. The month of April and May are almost free from western disturbances. The only source of rainfall in April is the pre-monsoon thunderstorms, the frequency of which is also much higher than in March [25].

A. Empirical Mode Decomposition Method

The Empirical Mode Decomposition (EMD) is recently developed method that is specifically designed to analyze the non-linear and non-stationary properties of a time series data [23], [26]. There is a straightforward assumption for EMD that the entire time series data must consist of simple intrinsic modes of oscillations. The mode, defined by the EMD method called intrinsic mode function (IMF).

Figure 1 shows the flowchart of IMF computation. EMD naturally separates non-linear oscillatory patterns of higher frequencies from those of lower frequencies and trend. EMD method separates time series into intrinsic oscillations using local temporal and structural characteristics of the data [17]. Each IMF should satisfy two basic conditions: (i) in the whole data set, the number of extrema and the number of zero crossing must be the same or differ at most by one, (ii) the mean value of the envelope defined by the local maxima and the envelope defined by the local minima is always zero. The first condition is similar to the narrow-band requirement for a stationary Gaussian process and the second condition is a local requirement induced from the global one, and is necessary to ensure that the instantaneous frequency will not have redundant fluctuations as induced by asymmetric waveforms. There exist many approaches of computing EMD [27], [28]. The following algorithm is adopted here to decompose the signal $x(t)$ into a set of IMF components.

a) Initialize the residue $r_0(t)=x(t)$ and index of IMF $k=1$
b) (i) set $g_0(t)=r_{k-1}(t)$ and $i=1$
(ii) Find the extrema (minima and maxima) of $g_{i-1}(t)$
(iii) Compute upper and lower envelopes $h_{i-1}(t)$ and $l_{i-1}(t)$
(iv) Find mean envelope $m_{i-1}(t)=[h_{i-1}(t)+l_{i-1}(t)]/2$
(v) Update $g_i(t)=g_{i-1}(t)- m_{i-1}(t)$ and $i=i+1$
(vi) Repeat steps (ii)-(v) until $g_i(t)$ being an IMF satisfying the above mentioned two basic conditions. If so, the k^{th} IMF $C_k(t)=g_i(t)$ and update residue $r_k(t)=r_{k-1}(t)-C_k(t)$

c) Repeat step (b) with the index of IMF $k=k+1$

At the end of EMD the time series $x(t)$ is represented as:

$$x(t) = \sum_{k=1}^{K} C_k + r_K \qquad (1)$$

where K is the number of IMF components and r_K is the final residue. The r_K monotonously converges to a constant or takes a function with only one maximum and minimum such that no more IMF can be derived.

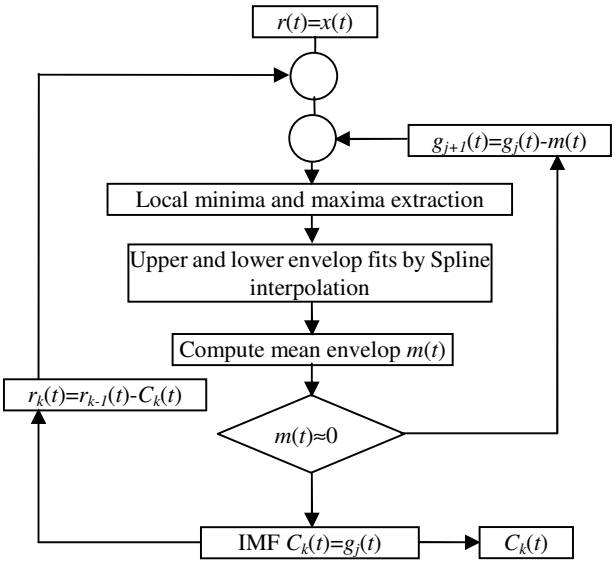

Fig. 1 sifting process to compute EMD

B. Instantaneous Frequency of IMF

The instantaneous frequency (IF) represents the signal's frequency at every time instance. IF is defined as the rate of change of the phase angle at the analysis time instant of the analytic version of the signal. Every IMF is a real valued signal and analytic signal method [29] is used to calculate the instantaneous frequency of each IMF.

The analytic (complex) signal corresponding to a real signal k^{th} IMF $C_k(t)$ is defined as:

$$z_k(t) = C_k(t) + j\hbar[C_k(t)] = a_k(t)e^{j\theta_k(t)} \qquad (2)$$

where $\hbar[]$ is the Hilbert transform operator, $a_k(t)$ and $\theta_k(t)$ are instantaneous amplitude and phase respectively of the k^{th} IMF. The Hilbert transform provides a phase-shift of $\pm\pi/2$ to all frequency components, whilst leaving the magnitudes unchanged [29]. The Hilbert transform of any arbitrary time-series $s(t)$ can be defined as:

$$\hbar[s(t)] = \frac{1}{\pi} \sum_{\delta=-\infty, \delta\neq t}^{\infty} \frac{s(\delta)}{t-\delta} \qquad (3)$$

With the definition, $s(t)$ and $\hbar[s(t)]$ together form a complex conjugate yielding the analytic signal $s(t) + j\hbar[s(t)]$. The analytic signal is advantageous to determine the instantaneous quantities such as energy, phase and frequency.

So the corresponding instantaneous frequency of the k^{th} IMF can easily be derived as:

$$\omega_k(t) = \frac{d\tilde{\theta}_k(t)}{dt} \qquad (4)$$

where $\tilde{\theta}_k(t)$ represents the unwrapped version of the phase vector $\theta_k(t)$. Using Eq. (2) and (4), the analytic signal associated with each of the IMFs and thus the instantaneous frequency of each of them is calculated. The overall effect of IF of all IMFs can be efficiently used as the time-frequency representation of the time domain signal.

C. Hilbert Spectrum and its Contribution

Hilbert Spectrum represents the distribution of the signal energy as a function of time and frequency. It is also designated as Hilbert amplitude spectrum $H(l,t)$ or simply Hilbert spectrum(HS). After performing the Hilbert transform on each IMF, the time series data can be expressed as:

$$x(t) = \Re\left(\sum_{k=1}^{K} a_k(t)e^{j\int\omega_k(t)dt}\right) \qquad (5)$$

where $\Re(.)$ represents the real part of the complex number and only K IMFs are taken into consideration leaving the residue [23]. This expression enables to represent the amplitude and IF as a function of time. To construct the Hilbert spectrum, the IF values are first normalized between 0 to 0.5. It reflects the Nyquist properties of the frequency domain representation. Each IF vector is multiplied by the scaling factor $\eta=0.5/(IF_{max}-IF_{min})$, where $IF_{max}=Max(\omega_1, \omega_2,\ldots,\omega_m,\ldots,\omega_K)$ and $IF_{min}=Min(\omega_1, \omega_2,\ldots,\omega_m,\ldots,\omega_K)$. The bin spacing of the HS is 0.5/B, where B is the number of desired frequency bins. The overall HS is expressed as the superposition of the individual IMFs' HSs defined as [23]:

$$H(l,t) = \sum_{k=1}^{K} H^{(k)}(l,t) \qquad (6)$$

where $H^k(l,t)$ is the HS of the k^{th} IMF. Hence, each element $H(l,t)$ of the overall HS is defined as the weighted sum of the instantaneous amplitudes of all the IMFs at l^{th} frequency bin.

$$H(l,t) = \sum_{k=1}^{K} a_k(t) w_k^{(l)}(t) \qquad (7)$$

where the weight factor $w_k^{(l)}(t)$ takes 1 if $\eta\times\omega_m(t)$ falls within l^{th} band, otherwise is 0. After computing the elements over the frequency bins, H represents the instantaneous signal spectrum in TF space as a 2D table. There are various forms to represent the Hilbert spectrum. If amplitude squared is more desirable commonly to represent energy density, then the squared values of amplitude can be substituted to produce the Hilbert energy

spectrum just as well. When the visualization is more preferable than the further analytic processing of the Hilbert spectrum, it can be presented as the smoothed version using some image filtering. It is noted that the time resolution of H is equal to the sampling rate and the frequency resolution can be chosen up to Nyquist limit.

The marginal spectrum defines a measure of total energy contribution from each frequency value. It represents the cumulated amplitude over the entire data length in a probabilistic sense. As we have already derived the Hilbert spectrum $H(l,t)$, the marginal spectrum $h(l)$ can be easily defined as:

$$h(l) = \int_t H(l,t)dt \qquad (8)$$

D. Efficiency of Decomposition

To measure the efficiency of the decomposition it should also be checked the orthogonality of the decomposition. The elements should all be locally orthogonal to each other. Higher the orthogonality corresponds to less amount of information leakage (cross terms of the data) between the components. The amount of leakage usually depends on the length of data as well as the decomposition method [30].

To check the orthogonality of IMFs from the EMD, an overall index of orthogonality, IO, is defined [31] as:

$$IO = \frac{1}{T}\sum_t \frac{1}{x^2(t)}\left(\sum_n^{K+1}\sum_k^{K+1} C_n(t)\cdot C_k(t)\right) \qquad (9)$$

where, n and k stand for the indices of IMFs. The residue is also included to evaluate the IO and that is why n and k are extended to $K+1$ instead of K. In the decomposition of the above described temperature data the overall IO value is only 0.00025.

The orthogonality can also be measured for any pair of components $C_n(t)$ and $C_k(t)$ as:

$$IO_{n,k} = \frac{1}{T}\sum_t \frac{C_n(t)\cdot C_k(t)}{C_n^2(t)+C_k^2(t)} \qquad (10)$$

The IMFs are interpreted as the basis vectors representing the data [24]. The EMD can also be treated as dyadic filter-bank [24], [27]. The focus in this study will be mainly on the most recent daily temperature records. The data analysis is performed by self written Matlab programs.

III. Results and Discussion

This study examines daily temperature data using by EMD which is the best-suited method to analyze. The 15 years daily basis temperature data and the decomposed the intrinsic mode function (IMFs) are shown in the following Figure 2. The EMD method is very effective on a climate data, the IMFs components are normally distributed and also energy density of IMF is Chi-square distribution. This result is consistent with the findings of Wu and Huang [24]. The results are statistically significance of information content for IMF components.

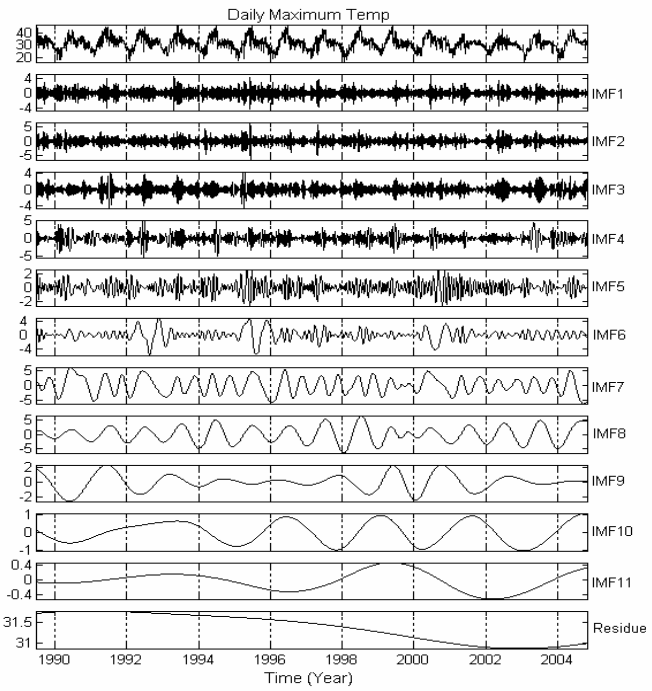

Fig. 2(a) EMD (IMF components and the final residue) of daily maximum temperature

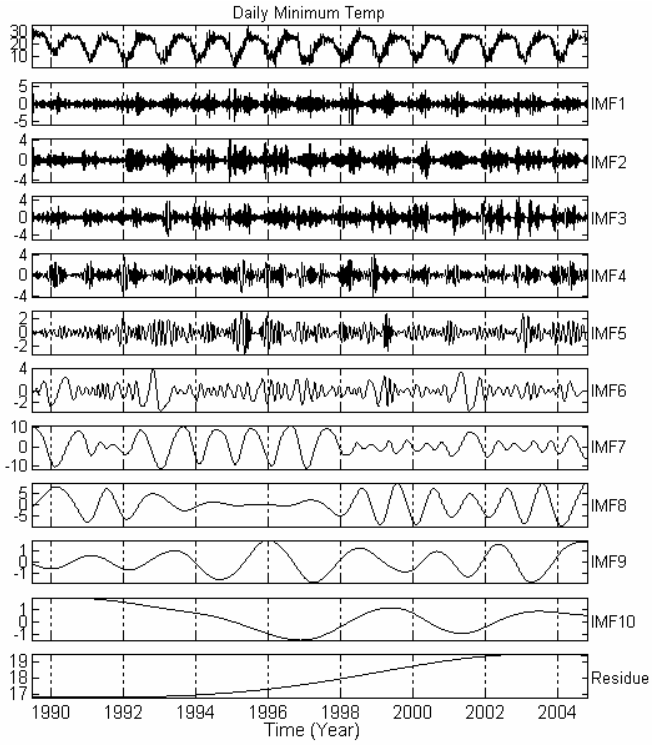

Fig. 2(b) EMD (IMF components and the final residue) of daily minimum temperature

Every IMF is a real valued signal and analytic signal method [29] is used to calculate the instantaneous frequency of the IMFs. The increasing anthropogenic impact to recent warming due to enhancement of greenhouse gasses could extend the

range of uncertainties in our prediction [32].

To build $H(l,t)$ in Eq. (7), the instantaneous frequency of each IMF is first scaled according to the given number of frequency bins. Figure 3 shows the Hilbert spectrum (HS) of the temperature data as shown in Figure 2 using 256 frequency bins. It represents that slow varying components in the data contains the most of the energy exhibited by the time series. Figure 2 show that strong inter-annual fluctuations exists both the maximum and minimum temperature. In addition, a rising tendency can also be seen from the time series. The graph of the residual series showed that overall fitted the data although a slight under-prediction of extreme values is evident (Fig. 2 & 5). The residual series are slightly dependent which may be due to small underlying trends caused by El Nino or climate change.

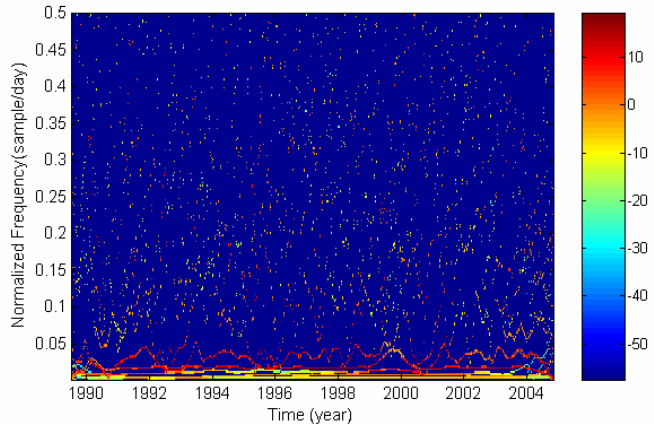

Fig. 3(a) Hilbert spectrum of maximum temperature using 256 frequency bins after 3x3 Gaussian filtering

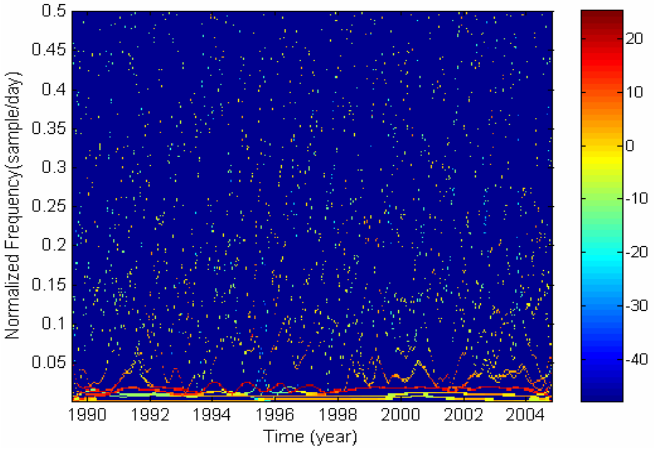

Fig. 3(b) Hilbert spectrum of minimum temperature using 256 frequency bins after 3x3 Gaussian filtering

The HS can visualize the data in time and frequency scales at the same time. Regarding the temperature data, HS makes clear about the distribution of the frequent and non-frequent temperature change at any time over the entire data length. This type of analysis is very much influential in the study of global warming. There are various forms to present the Hilbert spectrum, the popular form is the color map presentation as shown in Figure 3. Any point in the color map presentation corresponds to the energy in dB (determined by the color bar placed at the right side of the HS) at any specific time and frequency. In this study, the visualization of the Hilbert spectrum is improved by using 3x3 Gaussian filtering. However, in marginal Hilbert spectrum, the energy at the frequency (ω), means there is a higher likelihood that an oscillation with such a frequency exists.

A. IMF Component and its Probability Distribution

The study examines the probability distribution of individual IMFs shown in Figure 4. The probability density function for each IMF is approximately normally distributed, which is evident from the superimposed fitted normal distribution function. From the large sample theory, this fit is expected from Central Limit Theorem (CLT).

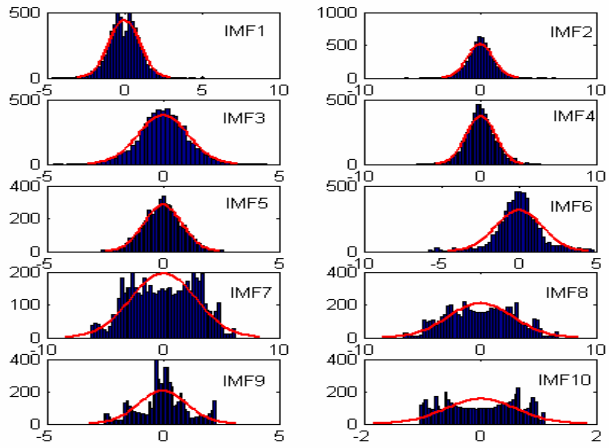

Fig. 4(a) probability distribution of the IMFs of maximum temperature

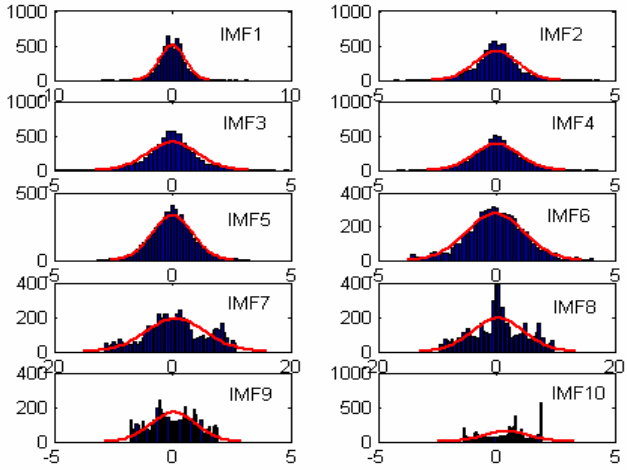

Fig. 4(b) probability distribution of the IMFs of minimum temperature

Definitely the deviation from the normal distribution function grows as the mode number increases (Fig. 4). This is because, in the higher frequency modes, the IMFs contain the smaller number of oscillations, therefore, the number of events decreases and the distribution becomes less smooth. When sample size is large, the IMFs of the higher frequency modes

will have more oscillations and the distribution will follow the normal distribution according to the CLT. The probability density function theory for a time series that has a normal distribution, its energy should have a Chi-square distribution [33]. The IMFs isolate physical processes of various time-scales and also give the temporal variation with the processes without resorting to the linear assumptions. They can also show the non-linear distortion of the waveform locally as discussed by Wu et al. [20]. Finally, IMFs can be effectively used to construct the time-frequency distribution in the form of a Hilbert spectrum, which offers details of the time variation of the underlying processes.

B. Efficiency Measure of IMF Components

A new technique for analyzing the special scaling structure of climatic fields has been discussed. An EMD analysis linearly decomposes temperature data into a finite set of IMFs, which are approximated by mutually orthogonal and sum of all IMFs including residue gets back to the original data with a negligible error.

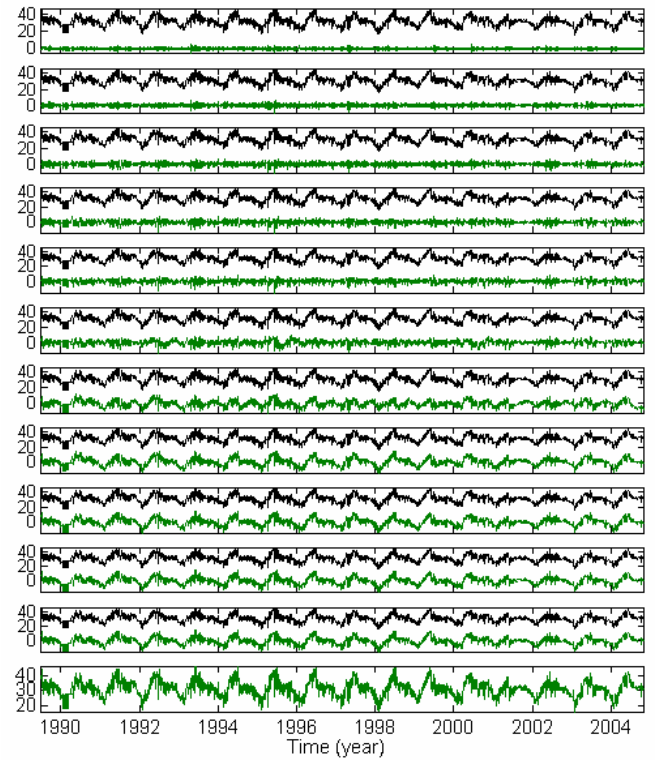

Fig. 5(a) stepwise reconstruction from EMD of maximum temperature; the upper one (black) is the original data and the lower one (green) is the stepwise reconstruction

With step-by-step adding of the IMF components, the sum of all components produces the time series which is very much similar to the original data as shown in Figure 5. Considering the entire data length, the maximum difference between the original and reconstructed data is of the order of 10^{-14}.

The elements of an efficient decomposition should be locally orthogonal to each other. Higher the orthogonality corresponds to less amount of information leakage between the elements. The amount of leakage usually depends on the length of data as well as the decomposition method [34].

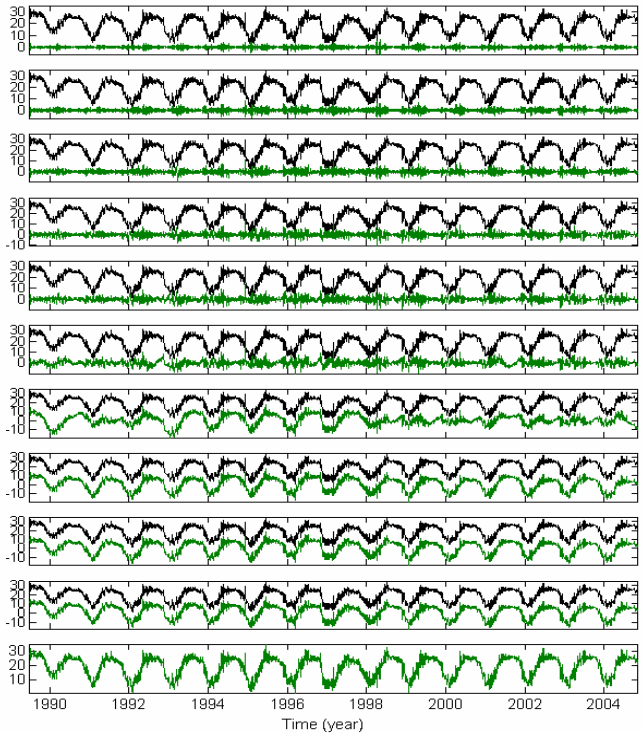

Fig. 5(b) stepwise reconstruction from EMD of minimum temperature; the upper one (black) is the original data and the lower one (green) is the stepwise reconstruction

The orthogonality values between all possible pairs of IMF components are shown in Figure 6. The *x* and *y* axis represent the indices of the decomposed components (IMF here) and the value of *z*-axis shows the index on orthogonality between the pair of components. It is noted that the maximum value of the index of orthogonality is of the order 8×10^{-5} which is very much less than the value of 0.001 proposed by Chang et al. [31].

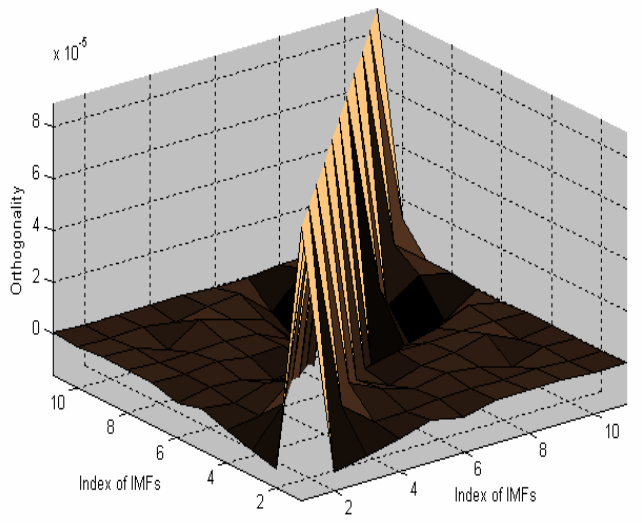

Fig. 6(a) orthogonality between the IMFs for maximum temperature

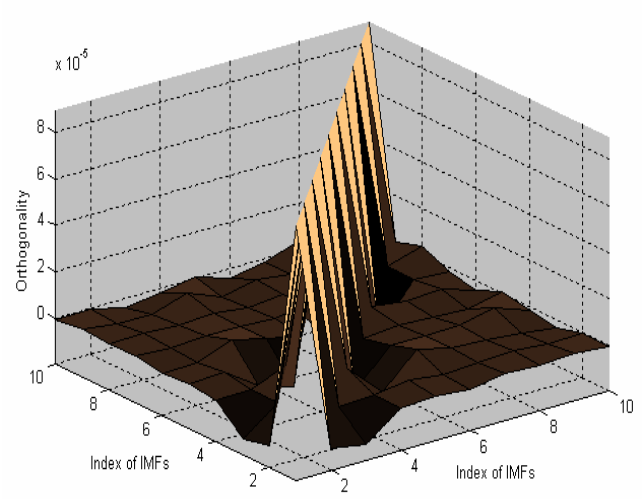

Fig. 6(b) orthogonality between the IMFs for minimum temperature

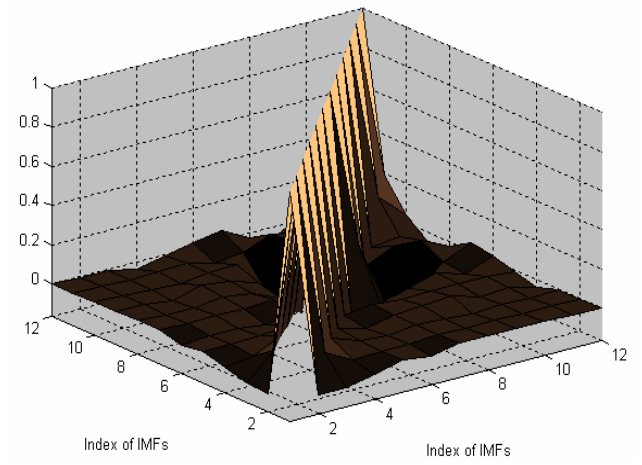

Fig. 7(a) correlation between IMFs for maximum temperature

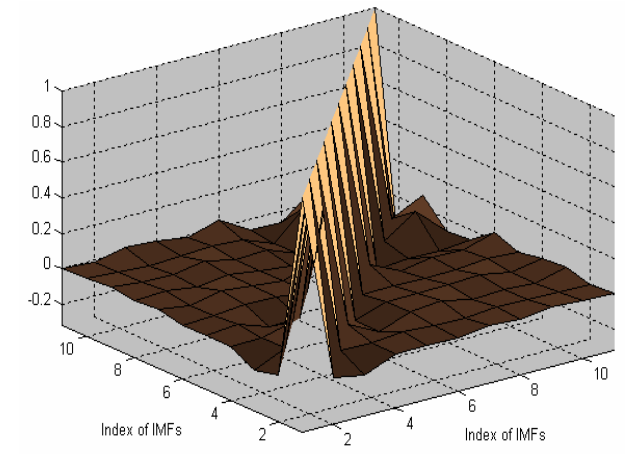

Fig. 7(b) correlation between IMFs for minimum temperature

By observing the completeness and orthogonality, the study concluded that the EMD method is well fitted to analyze the time series of temperature data. Figure 7 shows the correlation of IMFs for both maximum and minimum temperature. It indicates the IMF components are not correlated and hence a proper decomposition is achieved.

C. Computational Cost Benefit Analysis of IMF Components

Some other properties of the IMF components can also be useful to understand easily the analysis method of 15 years daily temperature data. The parameters values computed from the temperature data are listed in Table-I and Table-II. The mean period (calculated as the total number of extrema divided by the number of data samples) serves the information that how the EMD works as the filter-bank in data analysis. The percentage of energy content represents that how much energy of the data is contained by each IMF components and the variance offers the amount of information contained by the corresponding IMF. Finally the number of iteration required to compute individual IMF provides the idea about the computational cost of the analysis. The empirical findings are almost identical to those reported by Flandrin et al. [27].

TABLE- I
SOME VALUABLE PARAMETERS OF EMD FOR MAXIMUM TEMPERATURE

IMF	Mean Period	% of Energy	% of Variance	No. of Iteration
IMF1	0.3161	6.5599	3.9329	83
IMF2	0.1604	7.3642	4.9056	58
IMF3	0.0890	7.2141	4.5844	51
IMF4	0.0482	8.4089	6.4040	20
IMF5	0.0273	5.6837	2.6696	36
IMF6	0.0132	9.4468	9.0876	17
IMF7	0.0050	20.9887	31.0227	15
IMF8	0.0030	20.7931	31.2409	7
IMF9	0.0016	6.9380	4.3836	16
IMF10	0.0009	4.7700	1.5088	7
IMF11	0.0004	1.8325	0.2599	12

TABLE- II
SOME VALUABLE PARAMETERS OF EMD FOR MINIMUM TEMPERATURE

IMF	Mean Period	% of Energy	% of Variance	No. of Iteration
IMF1	0.3144	5.6123	2.1344	39
IMF2	0.1599	4.8425	1.5340	252
IMF3	0.0931	5.6961	2.1701	20
IMF4	0.0483	5.3102	1.7632	21
IMF5	0.0244	4.8265	1.3867	19
IMF6	0.0109	6.8594	2.7849	24
IMF7	0.0039	29.4860	48.7564	12
IMF8	0.0021	25.1336	36.0538	11
IMF9	0.0012	5.8507	1.6981	7
IMF10	0.0005	6.3827	1.7184	4

IV. CONCLUSIONS

The EMD method is highly data adaptive and efficient for nonlinear and non-stationary time series. The output of the analysis is also presented as a time-frequency-energy distribution, designated as the Hilbert Spectrum. The main superiority of this method are to apply the EMD method

yielding IMFs based on local properties of the signal and the instantaneous frequencies for complicated data sets, which eliminate the need for spurious harmonics to represent non-linear and non-stationary signals. The EMD is a new approach to many researchers in climate research. This study plays a vital role for analysis the properties of non-linear and non-stationary daily temperature time series data. This study focuses the relation between the temperature variability and global warming using EMD data analyzing method.

The results showed that most of the IMFs have normal distribution. Therefore, the energy density distribution of an IMF samples satisfy Chi-square distribution. The IMFs partitions the time series as a function of time-scale (frequency) in a statistically significant way. The residual series show that the data is overall fitted though a slight under-prediction of extreme values is occurred due to small underlying trends caused by El Nino or climate change. Some further statistical research would be needed to address these problems. The IMFs, each carrying its own time scales, could be used in statistical prediction of future climate scenarios. However, those climate predictions still remain as a challenge for future research.

REFERENCES

[1] Radic, V., Z. Pasaric and N. Sinik, "Analysis of Zagreb climatological data series using empirically decomposed intrinsic mode functions," *Geofizika*, 21, pp. 15-36, 2004.

[2] R. Voss, W. May and E. Roeckner, "Enhanched resolution modeling study on anthropogenic climate change: changes in extremes of the hydrological cycle", *International Journal of Climatology*, 22, pp. 755-777, 2002.

[3] K. E. Kunkel, R. A. Pielke and S. A. Changnon, "Temporal fluctuations in weather and climate extremes that cause economic and human health impacts: a review", *Bulletin of the American Meteorological Society*, 80, pp. 1077-1098, 1999.

[4] IPCC, *Climate change 1995: The science of climate change*, Cambridge University press, Cambridge, 1996.

[5] K. Dairaku, S. Emori, T. Nozawa, N. Yamazaki, M. Hara and H. Kawase, "Hydrological change under the global warming in Asia with a regional climate model nested in a general circulation model", *3rd International Workshop on Monsoons (IWM-III)*, 56, 2004.

[6] A. Markham, N. Dudley and S. Stolton, "Some like it hot. WWF International CH-1196", *Gland Switzerland*, reprint, 1994.

[7] B. C. Bates, S. P. Charles and J. P. Hughes, "Stochastic downscaling of numerical climate model simulations", *Environmental Modeling Software*, 13(3-4), pp. 325-331, 1998.

[8] B. Rajagopalan, U. Lall and M. A. Cane, "Anomalous ENSO occurrences: an alternative view", *Journal of Climate*, 10, pp. 2351-2357, 1997.

[9] B. Rajagopalan, U. Lall and M. A. Cane, "Comment on Reply to the Comments of Trenberth and Hurrell", *Bulletin of American Meteorological Society*, 80, pp. 2724-2726, 1999.

[10] D. E. Harrison and N. K. Larkin, "Darwin sea level pressure, 1876-1996: Evidence for climate change?" *Geophysics Review Letter*, 24, pp. 1779-1782, 1997.

[11] C. Wunsch, "The interpretation of short climate records, with comments on the North atlantic and Southern Oscillations", *Bulletin of American Meteorological Society*, 80, pp. 245-255, 1999.

[12] F. S. Mpelasoka, A. B. Mullan and R. G. Heerdegen, "New Zealand climate change information derived by multivariate statistical and artificial neural networks approaches", *International Journal of Climatology*, 21, pp. 1415-1433, 2001.

[13] D. R. Easterling, G. A. Meehl, C. Permesan, S. A. Changnon, T. R. Karl and L. O. Mearns, "Climate extremes: observations, modeling and impacts", *Science*, 289, pp. 2068-2074, 2000.

[14] T. Uchiyama, A. Noda, S. Yukimoto and M. Chiba, "Study of the estimate of new climate change scenarios based on new emission scenarios- IPCC AR4 experiments", *CGER's Supercomputer Activity Report*, Vol. 12-2003, pp. 51-58, 2005.

[15] M. J. Salinger and G. M. Griffiths, "Trends in New Zealand daily temperature and rainfall extremes", *International Journal of Climatology*, 21, pp. 1437-1452, 2001.

[16] K. Dairaku, S. Emori and T. Nozawa, "Hydrological projection over Asia under the global warming with a regional climate model nested in the CCSR/NIES AGCM", *CGER's Supercomputer Activity Report* Vol.12-2003, pp. 13-20, 2005.

[17] K. Coughlin and K. K. Tung, "Eleven year solar cycle signal throughout the lower atmosphere", *Journal of Geophysical Research*, 109, D21105, 2004.

[18] M. H. Glantz, R. W. Katz and N. Nicholls, "Teleconnections linking of worldwide climate anomalies", *Cambridge University Press*, 535, 1991.

[19] A. V. Fedorov and S. G. Philander, "Is El Nino Changing?" *Science*, 288, 2000.

[20] Z. Wu, E. K. Schneider, Z. Z. Hu and L. Cao, "The impact of of global warming on ENSO variability in climate records", *COLA Technical Report*, CTR 110, 2001.

[21] K. Dairaku, S. Emori, T. Nozawa, N. Yamazaki, M. Hara and H. Kawase, "Regional climate simulation over Asia under the global warming nested in the CCSR/NIES AGCM", *Symposium on Water Resource and Its Variability in Asia in the 21st Century*, 90-93, 2004.

[22] K. Dairaku, S. Emori, T. Nozawa, N. Yamazaki, M. Hara and H. Kawase, "Regional climate simulation over Asia under the global warming nested in the CCSR/NIES AGCM", *Symposium on Water Resource and Its Variability in Asia in the 21st Century*, pp. 756-764, 2004.

[23] N. E. Huang, Z. Shen, S. R. Long, M. C. Wu, H. H. Shih, Q. Zheng, N.-C. Yen, C. C. Tung and H. H. Liu, "The empirical mode decomposition and the Hilbert spectrum for nonlinear and non-stationary time series analysis", *Proc. of Royal Society London*, 454A, pp. 903-995, 1998.

[24] B. Z. Wu and N. E. Huang, "A study of the characteristics of white noise using the empirical mode decomposition", *Proc. R. Soc. Lond.*, 460A, 1597-1611, 2004.

[25] I. Sadhukhan, and U. K. De, "Pre-monsoon consecutive developments over Gangetic West Bengal during 1980-1989", *Indian Journal of Radio and Space Physics*, 27, pp. 102-109, 1998.

[26] P. Gloerson and N. Huang, "Comparison of interanual intrinsic modes in hemispheric sea ice covers and others geophysical parameters", *IEEE Trans. on Geosciences and Remote Sensing*, 41(5), pp. 1062-1074, 2003.

[27] P. Flandrin, G. Rilling and P. Goncalves, "Empirical mode decomposition as a filter bank", *IEEE Signal Processing Letters*, 11(2), pp. 112-114, 2004.

[28] M. C. Ivan, and G. B. Richard, "Empirical mode decomposition based frequency attributes", *Proceedings of the 69th SEG Meeting*, Texas, USA, 1999.

[29] M. Cooke, *Modeling Auditory Processing and Organisation*, Cambridge University press, 1993.

[30] N. E. Huang et al., "Application of Hilbert-Huang transform to non-stationary financial time series analysis", *Applied Stochastic Model in Business and Industry*, 19, pp. 245-268, 2003.

[31] C. Y. Chang, N. E. Huang and Z. Shen, "A statistically significance periodicity in the homestake solar neutrino data", *Chinese Journal of Physics*, Vol. 35 (6-11), pp. 818-831, 1997.

[32] IPCC, "Climate change 2001: The specific Basis, contribution of working group to the third assessment report of the intergovernmental panel on climate change", *Cambridge University Press*, Cambridge, UK and New York, USA, 2001.

[33] A. Papoulies, *Probability, Random Variable and Stochastic Processes*, Second Edition, Mc-Graw Hill, 1986.

[34] N. E. Huang, Z. Shen, and S. R. Long, "A new view of non-linear water waves: the Hilbert spectrum", *Annual Review of Fluid Mechanics*, 31, pp. 417-457, 1999.

Md. Khademul Islam Molla received B.Sc. and M.Sc. degrees in Electronics and Computer Science from Shahjalal University of Science and Technology, Bangladesh in 1995 and 1997 respectively. He joined in the same University as a lecturer in 1997. Then he joined as a lecturer and currently an assistant professor at the department of Computer Science and Engineering of the University of Rajshahi, Bangladesh.

Now he is a Ph.D. candidate under the department of Frontier Informatics at the University of Tokyo, Tokyo, Japan. His research interest covers speech and audio signal processing, blind source separation, statistical signal processing, neural signal processing, biomedical signal and image processing. He is a student member of the Institute of Electrical and Electronics Engineers (IEEE) since 2004.

Akimasa Sumi received Bachelor and Master Degrees in 1971 and 1973 respectively from the department of Physics, the University of Tokyo. He has awarded Degree of Science in Geophysics from the University of Tokyo in 1985. He has a long employment experiences as: Japan Meteorological Agency (1973-1979), Department of Geophysics, University of Hawaii (1979-1981), Japan Meteorological Agency (1981-1985), Associate Professor, Department of Geophysics, The University of Tokyo (1985-1991), Professor, Center for Climate System Research, The University of Tokyo (1991-present), Director of the Center for Climate System Research (1994-2004).

He is involved in many national and international scientific projects. He is a member of the Scientific Steering Committee of the TOGA (Tropical Ocean and Global Atmosphere), WCRP (World Climate Research Programme) during 1985-1994 and Joint Scientific Committee of WCRP during 1997-2002. His research interest focuses on Numerical Prediction, Monsoon meteorology, Climate Dynamics, and Climate Modeling and published more than 50 scientific papers.

M. Sayedur Rahman received B.Sc. (Honours) and M.Sc. degree in statistics from University of Rajshahi. He also received M. Phil. degree from Department of Agricultural and Environmental Sciences, University of Newcastle upon Tyne, U.K. and Ph.D. degrees from University of Rajshahi. He was joined as a lecturer in 1988, Department of Statistics, University of Rajshahi, and subsequently he promoted as Professor in 2003.

At present, he is working as a visiting Professor, Center for Climate System Research, The University of Tokyo. He is actively involved in teaching and research. Professor Rahman`s main research areas are the simulation modelling, applied statistics, environmental statistics and impact of global warming. He is involved in different projects and research groups. He has also authored and co-authored more than 35 research and review papers.